

Large algebraic connectivity fluctuations in spatial network ensembles imply a predictive advantage from node location information

Matthew Garrod and Nick S. Jones

Department of Mathematics, Imperial College London.

(Dated: June 16, 2022)

A Random Geometric Graph (RGG) ensemble is defined by the disordered distribution of its node locations. We investigate how this randomness drives sample-to-sample fluctuations in the dynamical properties of these graphs. We study the distributional properties of the algebraic connectivity which is a graph property linked to diffusion and synchronization timescales. We use numerical simulations to provide the first characterisation of the algebraic connectivity distribution for RGG ensembles. We find that the algebraic connectivity can show fluctuations relative to its mean on the order of 30%, even for relatively large RGG ensembles ($N = 10^5$). We demonstrate that the factors driving these fluctuations vary between RGG ensembles with different choices of dimensionality, boundary conditions and node distributions. We also find that the behaviour of the fluctuations is non-monotonic as a function of key system parameters with a magnitude which can increase with system size. We analyse the within-ensemble correlations between the algebraic connectivity and various graph structural properties and show that ensemble fluctuations in the minimum degree of graphs and density inhomogeneities in the distribution of nodes can both drive fluctuations in the algebraic connectivity. We also derive a closed-form expression for the expected algebraic connectivity for RGGs with periodic boundary conditions for general dimension.

I. INTRODUCTION

A. Motivation

Networks frequently show spatial or metric structure where nodes possessing similar attributes are more likely to share a connection [1, 2]. A general framework for modelling networks where edge formation is dependent on continuous node attributes is the Soft Random Geometric Graph [3–5] or Spatially Embedded Random Network [2]. In these models node positions, X_i , for $i = 1, \dots, N$ are sampled in some chosen domain, \mathcal{D} , according to some distribution $P(\cdot)$. Connections between nodes are then drawn independently with a probability which is a function of their Euclidean distance. This is typically expressed via some connection probability function $f(r)$ which specifies the probability that two nodes separated by a distance, r , are connected.

Models of within this class have been used in a diverse range of applications including: social networks [6–8], wireless communications networks [4, 9, 10], spatially constrained networks in the brain [11, 12] and transport networks [13]. However, in practice, the amount of information that we possess about the graph structure can vary significantly. For example, in some cases, we might possess microscopic data about individual nodes, such as, geographic locations [7, 8] or socio-economic coordinates [14] of people or organisations in a social network. In other cases we may possess coarse-grained data describing the density of individuals. For instance, population density contained within census data which has been used as an input for models of social networks [15, 16] and transportation networks [13]. Furthermore, even when we do not possess data about individual nodes, we can often obtain their relative positions in some latent embedding space [17]. In fact, it has been found that many

complex networks can be well represented by embedding the nodes in a hyperbolic space [18–20].

We can expect higher levels of detail to be more costly: in social networks, conducting a survey to obtain microscopic details about individuals will carry some cost, whereas census data containing distributions of individuals traits across populations may be freely available. In a particular situation it becomes relevant to ask: *what level of information do we need to know about the node attributes in order to determine the structural or dynamical properties of the network to the desired degree of accuracy?* In this paper we answer the above question by studying ensemble variability in spatial network ensembles. By ensemble variability we refer to the degree to which different graphs drawn from the same random graph ensemble vary in their structural and dynamical properties.

The choice of $f(r)$ varies widely between different applications [7, 8, 11, 12]. We focus on the case of the Random Geometric Graph (RGG) for which two nodes i and j are connected if $|X_i - X_j| \leq R$ (Figure 1). Studying ensemble variability in RGGs allows us to characterise how randomness in the node locations influences variability in the structural and dynamical properties of the network. This in turn allows us to identify the level of knowledge (e.g node distribution or precise knowledge of node locations) required to make accurate predictions of structurally and dynamically relevant properties.

B. Problem Setup

Suppose we are interested in a network property, q . For a particular random geometric graph ensemble q will be a random variable with an expected value $\mathbb{E}(q)$, standard deviation $\sigma(q)$ and distribution $\mathcal{P}_q(q)$. Given $P(\cdot)$, N and

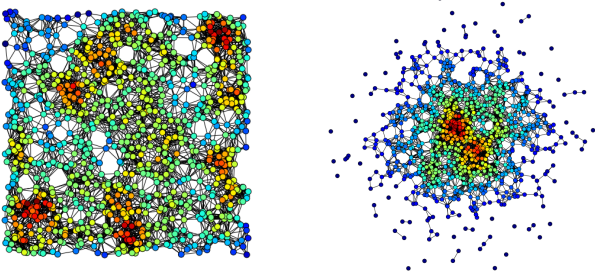


FIG. 1. Examples of RGGs with $N = 1000$ for different node distributions. Shows the case of a uniform node distribution in $[0, 1]^2$ with $R = 0.082$ (left) and 2D Gaussian node distribution in \mathbb{R}^2 with unit variance and zero mean with $R = 0.281$ (right).

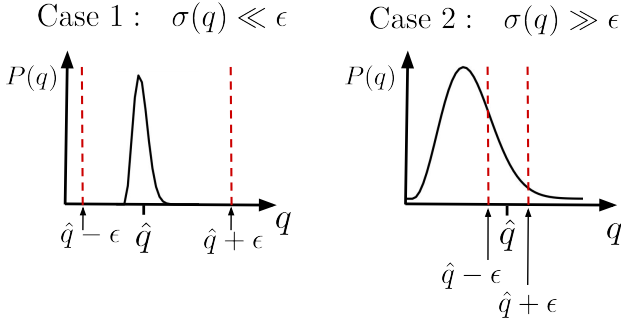


FIG. 2. Figure illustrating how ensemble variability of a graph property, q , relates to our ability to be able to estimate it to within some threshold value, ϵ . Case 1 shows an example where the ensemble variability of q is much smaller than the desired precision, ϵ . Case 2 illustrates the case where the ensemble variability of q is much larger than the desired precision. In the former case it will be possible to make estimates of the true value of q to the desired precision by taking the value of q from any graph sampled from the ensemble.

R it is possible to draw representative members from the ensemble in order to estimate q . For some RGG ensembles, we may also be able to estimate $\mathbb{E}(q)$ analytically given knowledge of the node distribution and connection radius.

Suppose the true value of q for a graph is given by q^* . In practice we may want to predict the value of q for a particular RGG to within some threshold ϵ ie. the predicted value \tilde{q} satisfies: $\tilde{q} \in [q^* + \epsilon, q^* - \epsilon]$. Whether this is possible given knowledge of $P(\cdot)$ alone will depend on the standard deviation of the distribution of q . For example, there are two limiting cases (See Figure 2):

1. **Case 1:** If $\sigma(q) \ll \epsilon$, the vast majority of values of q sampled from $\mathcal{P}_q(q)$ will lie within the desired region. As a consequence, a sensible guess for q^* could be made by taking $\mathbb{E}(q)$.

2. **Case 2:** If $\sigma(q) \gg \epsilon$, then samples from the distribution $\mathcal{P}_q(q)$ are likely to be uninformative of the value of q^* for the particular graph.

In the later case knowledge of the set of node positions $\underline{X} = (X_1, X_2, \dots, X_N)$ will be of utility since it will allow us to generate a network for which we can compute q .

The particular choice of ϵ is subjective and depends on the application. In this work we investigate the case where $\epsilon \approx \mathbb{E}(q)$, that is, we are interested in when it will be possible to predict q to within a threshold determined by the length scale of the mean of the distribution.

Given the above choice of ϵ , a relevant metric to study when comparing the typical width of $\mathcal{P}_q(q)$ for different network ensembles is the *coefficient of variation* (CV). The CV is defined as the standard deviation of a distribution divided by its mean: $CV(q) = \frac{\sigma(q)}{\mathbb{E}(q)}$. If $CV(q) \approx 0$ then $\mathbb{E}(q)$ will be sufficient to predict q for most ensemble members. In contrast, if $CV(q)$ is relatively large, then knowledge of $\mathbb{E}(q)$ will not be sufficient in order to make precise predictions about the value of q for a particular ensemble member.

The notion of whether a network property is well-represented by its mean across random network ensembles has been studied in the past in [21] and [22]. They refer to a property which can be well represented by its ensemble average as being *ensemble averageable*. They studied the degree to which certain spectral properties of networks are ensemble averageable in scale-free and real world network ensembles. Technically speaking, a property is ensemble averageable if $\sigma(q)$ remains finite in the thermodynamic limit. However, since most real world networks are large but finite we instead focus on identifying cases where $CV(q)$ remains large (for example fluctuations on the order 5 – 10% at least) for the ranges of N studied.

C. The Algebraic Connectivity

Networks can be studied via the adjacency matrix, A , for which $A_{ij} = 1$ if nodes i and j share an edge and 0 otherwise, and the Laplacian matrix, L , which has elements $L_{ij} = \delta_{ij}(\sum_j A_{ij}) - A_{ij}$. The smallest non-zero eigenvalue of this matrix, μ_2 , is commonly known as the *algebraic connectivity*. This quantity is connected to both dynamical properties such as the characteristic timescale of diffusion [23] and synchronizability [24, 25] as well as a metric of how difficult it is to partition the network into two components [26]. In the study of wireless communications networks, the algebraic connectivity is related to the time required for linear consensus algorithms to run to completion and their total energy consumption [27–29]. As a consequence, there are numerous cases in which we might want to estimate the algebraic connectivity of large networks.

The algebraic connectivity of RGGs has been studied in [30] where they find a bound on its value in terms of

the number of nodes and the domain size. In addition, in [28] they derive an analytic approximation for the algebraic connectivity of $2d$ RGGs with periodic boundary conditions. However, to our knowledge, there have been no studies of the distribution of μ_2 values, $\mathbb{P}(\mu_2)$, in RGG ensembles with fixed parameter values. We will also consider the effect of varying the spatial dimension of the system as many complex networks, such as large scale social networks, can be represented using a moderate number of dimensions [31].

The algebraic connectivity distribution has been studied in [22] for network ensembles modeled on real world networks and in [32] for stochastic block models. In both cases it is reported that the distribution of values can be ‘broad’ or of high variance. However, neither study addresses the question of how the width and form of $\mathbb{P}(\mu_2)$ depends on the parameters of the random graph model.

The eigenvalue spectra of the adjacency matrix for RGGs has been studied in [33–35]. In the former case they show that the spectrum shows some universal features also seen in the spectral distributions of other random network models, while in the latter it is shown how the spectral properties can be related to the frequency of occurrence of certain subgraphs (also known as *motifs*) in the network. However, no research so far has focused the distributions of individual eigenvalues in RGGs which is the subject of the present manuscript.

The algebraic connectivity is inversely proportional to the characteristic timescale of linear diffusion [23] and related to the timescale of synchronization [24, 25]. As a consequence, we might expect it show some covariation with network properties which measure the typical separation between network nodes. The average shortest path length, L , is defined by:

$$L = \frac{1}{N(N-1)} \sum_{i,j \in V} d(i,j), \quad (1)$$

where $d(i,j)$ is the shortest path between nodes i and j and V is the set of vertices in the network. We might also expect the minimum degree of the graph, κ_{\min} , which is known to be informative of μ_2 in Erdős-Rényi (ER) random graphs [36]. L is distinct from κ_{\min} since the former tell us about the global structure of the network, while κ_{\min} is a local property relating to the single node with fewest links. Furthermore, L is obtained by averaging over all node pairs, while κ_{\min} is obtained by taking the most extreme value of the distribution of degrees for a particular graph.

The algebraic connectivity of a disconnected graph is equal to zero. In this work we will consider the value of μ_2 for the largest connected component (LCC) of the graph. The values of other graph properties (e.g κ_{\min} and L) will also correspond to those for the LCC unless otherwise specified.

In some of the following sections we study the covariation between μ_2 and the other network properties. This can be quantified by computing Spearman’s rank correlation. This metric measures the extent of the monotonic

correlation between two variables. We will denote the Spearman correlation between two variables X and Y as $\rho(X,Y)$.

D. Summary of Results

In this paper we show that $CV(\mu_2)$, which measures the fluctuations in μ_2 relative to the ensemble mean, can become large (> 0.3) in several regions in parameter space. This implies that the μ_2 of a typical graph may not be well represented by the corresponding ensemble mean. We consider the effect of varying the parameters: N , the number of nodes, κ the average nodal degree and d , the embedding dimension, on the statistical properties of μ_2 . We control the connectivity of the system in terms of a parameter $C = \frac{\kappa}{\log(N)}$ (this choice of scaling is motivated in section II). We find that $CV(\mu_2)$ shows a non-trivial dependence on the system parameters. For example, it can show non-monotonicity with respect to the values of C (or κ), N and d .

We have identified five leading factors which can drive fluctuations in μ_2 . In RGGs with uniform node distributions $CV(\mu_2)$ can increase due to: small system size, sampling from ensembles with κ values below the connectivity threshold, fluctuations in κ_{\min} and variability in the number of low degree nodes. The choice of boundaries of the embedding domain can also have an impact on the structural properties of the graph, which can in turn lead to larger values of $CV(\mu_2)$. For RGGs with Gaussian distributions of nodes the value of $CV(\mu_2)$ is significant for a wide range of parameter values. In this case we demonstrate that the fluctuations in μ_2 due to the chance occurrence of weakly connected subgraphs.

In addition to investigating ensemble variability of μ_2 , we also provide an analytic formula for the $\mathbb{E}(\mu_2)$ in RGGs in $[0,1]^d$ with periodic boundary conditions for arbitrary d . This is an extension of the work in [28]. We show that the formula derived provides a good approximations for the algebraic connectivity of RGGs for finite N .

The remainder of the manuscript is laid out as follows. In section II we discuss the methodology used to generate RGGs with a fixed mean degree and the computation of eigenvalues for large matrices. In section III we explore how $\mathbb{E}(\mu_2)$ and $CV(\mu_2)$ vary as a function of the system parameters in different RGG ensembles with uniform node distributions. Section III C explores the network structural features that drive fluctuations in μ_2 . In section IV we analyse the factors driving sample-to-sample fluctuations in RGGs with Gaussian node distributions by considering the properties of the eigenvector associated with μ_2 . Finally, section V provides a discussion of the results and their implications for the utility of knowing node locations in spatial networks.

II. METHODOLOGY

A. Generation of RGG Ensembles with Given Expected Degree

In order to compare different RGG ensembles it is helpful to be able to specify the mean degree of the ensemble. In this section we assume that node positions lie in the domain $[0, 1]^d$ with either solid or periodic boundaries. In the high density limit the mean degree of the network can be computed by estimating the number of points which fall within the connection radius of a randomly chosen node. For the case where the domain of interest is of unit volume the probability of some node j falling within the connection radius of a node i is given by the volume of the ball of radius R in d dimensions. Multiplying this quantity by the number of remaining nodes in the network gives us an estimate for the mean degree of the form:

$$\tilde{\kappa} = (N - 1) \frac{\pi^{\frac{d}{2}}}{\Gamma(\frac{d+2}{2})} R^d. \quad (2)$$

Inverting this formula allows us to obtain an approximate expression for the connection radius required to generate RGG ensembles with true mean degree, κ , in d dimensions for a network with N nodes:

$$R = \frac{1}{\sqrt{\pi}} \left(\frac{\kappa}{N - 1} \Gamma\left(\frac{d+2}{2}\right) \right)^{\frac{1}{d}}. \quad (3)$$

This approach works well in practice for RGGs with periodic boundary conditions. However, for RGGs generated in $[0, 1]^d$ with solid boundaries the true mean degree of the ensemble, κ , will in general be lower than the value of $\tilde{\kappa}$ due to the presence of isolated nodes at the boundaries. In theory it is possible to compute the radius required to obtain a given expected mean degree using techniques described in [4] and [37]. However, this problem becomes analytically intractable for higher dimensional systems as the number of boundary, edge and corner terms in the integration will increase dramatically. Consequently, we must rely on a different procedure to generate RGGs with the desired mean degree for the solid boundary case.

Equation (3) can also perform poorly for higher dimensional systems with periodic boundaries. If $R > 0.5$ for a node embedded in $[0, 1]^d$ then the connectivity radius will cross over the periodic boundary and overlap with itself. As a consequence, the volume contained within the ‘ball of connectivity’ will be smaller than that required to obtain the desired mean degree. For small d this is not usually an issue since we require a large value of κ for the wrap-around effect to occur. However, for the case of higher dimensions, this wrap-around effect can occur for RGGs with relatively small mean degrees. For example, if we take $N = 10^4$, $\kappa = 20.0$, $d = 15$ then using (3) gives $R \approx 15.8$ which indicates that the ‘ball of connectivity’ can wrap-around the periodic domain multiple times despite only filling only a very small fraction of the entire volume.

Estimation of required radius via sampling from the distance distribution. Given the above it is necessary to have a systematic approach that allows us to identify values of R which correspond to desired choices of κ . In order to do this we use a method which relies on fixing the number of edges in the network (a similar approach is used in [38]). The mean degree of a network is related to the number of edges, E , by:

$$\kappa = \frac{2E}{N}. \quad (4)$$

Given a set of points X_1, X_2, \dots, X_N in some domain we can compute a sorted set of pairwise Euclidean distances: $\delta_1 \leq \delta_2 \leq \dots \leq \delta_P$ where $P = \frac{N(N-1)}{2}$. To generate an RGG with E edges we require that at least E pairs of nodes lie within a Euclidean distance R of each other. Consequently, the connection radius required to generate a graph containing E edges will satisfy the inequality:

$$\delta_E < R < \delta_{E+1}. \quad (5)$$

Choosing a value of R which falls within this range will allow us to construct an RGG with a mean degree of κ for the specified set of positions.

Choosing the connection radius based on the distance distribution allows us to generate an RGG with the desired mean degree without having to explicitly generate the graph first. This approach also has the advantage that it allows us to identify the desired value of R for any choice of domain or node distribution for which we can compute pairwise distances.

Subsampling approach for larger networks. For a network containing N nodes we must store an array of $\frac{N(N-1)}{2}$ pairwise distances. This will become computationally infeasible for large N . Consequently, for a given N and κ we estimate R by drawing a smaller sample from the node distribution of $M = 1000$ positions which gives us access to an array of 499,500 samples from the distribution of distances. Given this we can approximate the connection radius with:

$$R \approx \delta_{\lfloor E' \rfloor}, \quad (6)$$

where $\lfloor x \rfloor$ denotes the floor function and $E' = \frac{2E}{N(N-1)} \frac{M(M-1)}{2}$ and we have ordered the distances according to their size. We have used numerical simulations to confirm that the above methodology produces RGG ensembles with mean degrees close to the desired mean degree.

For the remainder of this paper we will report the parameter κ used as an input to generate the mean degree as opposed to the empirically observed mean degrees of samples. We choose this as the observed ensemble mean degree will be slightly different for each graph drawn from an RGG ensemble. However, for sufficiently large sample size the ensemble mean will lie very close to the actual value.

Percolation and Connectivity. Consider an RGG in some domain \mathcal{D} with fixed, d , N and some choice

of $P(\cdot)$. As we increase κ we will observe two significant transitions. For small κ , RGGs sampled from the ensemble will consist of small disconnected clusters of nodes. Once we pass a certain threshold we will find that a macroscopic fraction of the nodes lie within the largest connected component (LCC) of the graph. The transition to this regime is commonly referred to as the percolation transition. If we increase κ further we will eventually reach a point where all nodes lie within the LCC with high probability. We will refer to such a graph as being connected. The dominant contribution to the connectivity probability in RGGs comes from single isolated nodes [37]. As a consequence, the value of κ required to achieve connectivity is highly sensitive to the shape of the domain and presence of boundaries.

In order to achieve connectivity in RGGs the value of κ must be scaled logarithmically with N [39]. This can be achieved by setting:

$$\kappa = C \log(N), \quad (7)$$

where C is a positive constant. The connectivity threshold in the large N limit is $C = 1$. Therefore, graphs with $C > 1$ are highly likely to be connected, while those with $C < 1$ are most likely to be disconnected. Tuning C allows us to specify how far above the threshold of connectivity a given graph ensemble is.

The majority of ensembles studied in this paper are such that the number of nodes in the LCC, N_{LCC} , is equal to or close to N . We take this as justification for reporting the parameter N rather than N_{LCC} for the majority of results. The exception to this is when $C < 1$, in which case we will observe fluctuations in N_{LCC} . This effect is discussed briefly in III C.

B. Simulation Methodology

RGGs were generated using code in the Python programming language. Adjacency matrices for the graphs were stored in sparse matrix formats. A significant speed up in the procedure used to generate RGGs was obtained by using the Cython package for Python. In addition to this, efficient computation of nearest-neighbour distance was implemented using a KD-Tree based data structure for storing the node positions. Using this methodology it was possible to efficiently draw adjacency matrices for RGGs with sizes of up to $N \approx 10^5$. The eigenvalues of large sparse Laplacian matrices were computed using functions from the ARPACK toolbox in the Python programming language [40].

III. ENSEMBLE AVERAGEABILITY OF THE ALGEBRAIC CONNECTIVITY

In this section we explore how $\mathbb{E}(\mu_2)$ and $CV(\mu_2)$ vary as a function of the system parameters for different RGG ensembles. We consider three distinct RGG ensembles:

1. **Periodic Boundaries:** Node positions drawn from a uniform distribution in $[0, 1]^d$ with toroidal boundary conditions.
2. **Solid Boundaries:** Node positions drawn from a uniform distribution in $[0, 1]^d$ with solid boundaries.
3. **Gaussian Node Positions:** Node positions drawn from bivariate Gaussian density:

$$f(x_1, x_2) = \frac{1}{(2\pi)^{\frac{d}{2}}} e^{-\frac{(x_1^2 + x_2^2)}{2}}, \quad (8)$$

on \mathbb{R}^2 .

The motivation for considering periodic RGGs is that they are often studied as a means of making the mathematics more analytically tractable by removing boundary effects (for example in [28]). Comparing periodic and solid boundaries allows us to understand when boundaries are important in determining network properties. Studying the case of Gaussian RGGs has two motivations. Firstly, it allows us to understand how non-uniformity in the node locations effects the network properties, and secondly, spatial networks with Gaussian distributed node locations have been studied in the case of latent position inference [41] meaning that any results obtained will be practically applicable.

A. Behaviour of $\mathbb{E}(\mu_2)$

The value of $\mathbb{E}(\mu_2)$ is informative about how well connected the graph is as a whole. An analytic approximation for $\mathbb{E}(\mu_2)$ is derived in [28] for RGGs with node position in $[0, 1]^2$ with toroidal boundary conditions. In Appendix B we extend this approach to the case of general d in order to obtain an approximation of the form:

$$\mu_2 \approx \kappa - NR^{\frac{d}{2}} J_{\frac{d}{2}}(2\pi R), \quad (9)$$

where J_α is a Bessel function of the first kind of order α . This approximation holds for the case of $N \rightarrow \infty$, however, as we show below, it provides a good approximation to the behaviour of $\mathbb{E}(\mu_2)$ for the case of finite N .

Higher dimensional RGGs have similar properties to ER graphs [42]. In [36] they derive the mean and variance of $\mathbb{P}(\mu_2)$ for ER networks by approximating μ_2 by κ_{\min} . This motivates us to compare the values of μ_2 observed to the ensemble mean value of the minimum degree, $\mathbb{E}(\kappa_{\min})$. Figure 3 shows the behaviour of $\mathbb{E}(\mu_2)$ as a function of d . Also shown is the behaviour of $\mathbb{E}(\kappa_{\min})$ for the corresponding graph ensembles as well as the predictions of $\mathbb{E}(\mu_2)$ made based on equation (3) of [36] and equation (9).

For RGGs with periodic boundaries, as d is increased for fixed N and κ , we observe an increase in the value of $\mathbb{E}(\mu_2)$ from an initially small value to one which approaches $\mathbb{E}(\kappa_{\min})$. In this regime, both the analytic approximation of [36] and that from equation (9) can be

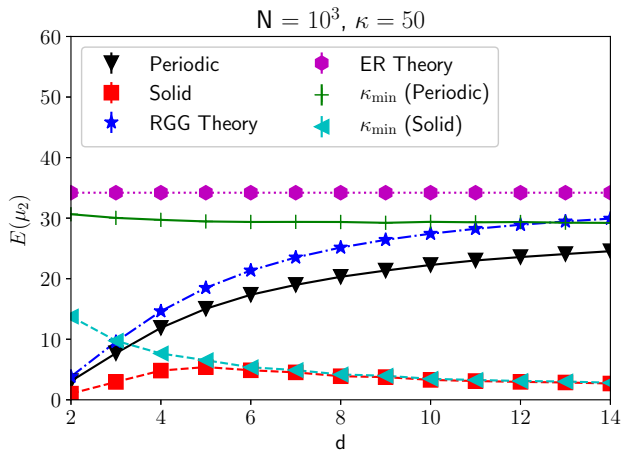


FIG. 3. **In high dimensional RGGs the behaviour of μ_2 can be accounted for by that of κ_{\min} .** Plot showing the behaviour of $\mathbb{E}(\mu_2)$ for RGGs in $[0, 1]^d$ as a function of dimensionality for RGGs with periodic and solid boundaries (black triangles and red squares). Also shown are values of $\mathbb{E}(\kappa_{\min})$ for the same ensembles (green crosses and cyan triangles) and theoretical predictions of μ_2 made using (9) (blue stars). For periodic RGGs the simulated value of $\mathbb{E}(\mu_2)$ as a function of d closely matches that of the theoretical prediction obtained using equation (9). For larger values of d both of these values approach the observed value of κ_{\min} and appear to be bounded by the theoretical value of $\mathbb{E}(\kappa_{\min})$ for ER graphs (purple circles). For solid RGGs the observed value of $\mathbb{E}(\mu_2)$ (red squares) is well approximated by the observed value of $\mathbb{E}(\kappa_{\min})$ (cyan triangles). Results are averaged over 200 simulations. Error bars are smaller than the symbol size.

used to approximate the value of μ_2 . For RGGs with solid boundaries the algebraic connectivity is typically much lower than for the periodic case. Despite this, we see that in higher dimensions the behaviour of $\mathbb{E}(\mu_2)$ for RGGs with solid boundaries is also well approximated by the estimated value of $\mathbb{E}(\kappa_{\min})$.

The results shown in Figure 3 demonstrate that the average value of μ_2 can be accounted for by κ_{\min} in higher dimensional RGG ensembles. In this regime it is also possible to account for the fluctuations in μ_2 across the ensemble by considering the fluctuations in κ_{\min} . Figure 4 shows scatter plots of μ_2 , L with the points coloured according to the κ_{\min} of the graph for RGGs with $N = 10^4$. This illustrates that different factors can drive sample-sample fluctuations in μ_2 for RGG ensembles in different dimensions. In lower dimensional systems, fluctuations in L can be important, while in the case of higher dimensional systems (Figure 4c) the value of μ_2 for a particular graph is determined almost entirely by its minimum degree. The factors which influence the variability in μ_2 are the topic of the next section.

B. Behaviour of $CV(\mu_2)$

We now consider how the size of the fluctuations in μ_2 , measured using $CV(\mu_2)$, vary as a function of the system parameters. Figure 5 shows heat plots of $CV(\mu_2)$ as a function of the network size, N and scaling parameter, C , for different RGG ensembles. The dependence on of $CV(\mu_2)$ on the system parameters appears to vary significantly between the different RGG ensembles. The results shown in figure 5 are all for the case where $C > 1$. This threshold does not necessarily ensure full connectivity in RGGs with solid boundaries, however, in practice, we have observed $N_{LCC} \approx N$ for the results presented in Figure 5.

We now briefly discuss the effect of the different parameters on the behaviour of $CV(\mu_2)$. From Figure 5 it is clear that the effects of the different parameters cannot necessarily be treated in isolation and that rich phenomena are observed. Nevertheless, we observe the following broad trends:

1. **Effect of System Size, N .** For small values of N , $CV(\mu_2)$ decreases with system size. This result agrees with our initial intuition as we expect the properties of a system to be better represented by the ensemble mean as the system size increases. However, for $N > 10^4$ we observe that $CV(\mu_2)$ begins to increase. An explanation for this initially surprising result is presented in section III C.
2. **Effect of the mean degree, κ .** The effect of varying the connectivity of the graph is encoded either in the mean degree κ or C . In the majority of cases we observe that increasing κ or C leads to a decrease in $CV(\mu_2)$. The exception to this can occur when $C \approx 1$. For example, for periodic RGGs with $d = 10$ (Figure 5c) we observe non-monotonicity in $CV(\mu_2)$ as a function of C for fixed N indicating that the statistical properties of the graph ensemble can be sensitive to the choice of average degree. We also observe similar non-monotonicity for the solid boundary case (Figure 5f), however, this occurs at much larger values of C .
3. **Effect of boundaries and dimensionality.** For RGGs with periodic boundaries increasing d makes the resulting graphs more ‘ER-like’ [42]. The result of this is that fluctuations in μ_2 are governed by those in κ_{\min} . This appears to lead to an increase in $CV(\mu_2)$ with d . Adding solid boundaries to RGGs in $[0, 1]^d$ decreases the connection probability for nodes close to the edge of the domain. The result of this is that graphs within the ensemble will typically have a smaller value of κ_{\min} . This effect makes little difference to the results for the case of $d = 2$ (Figures 5a and 5d), however, it is important in higher dimensions. In both cases increasing d leads to an increase in the range of values with large $CV(\mu_2)$. Although, this increase is more significant for RGGs with solid boundaries.

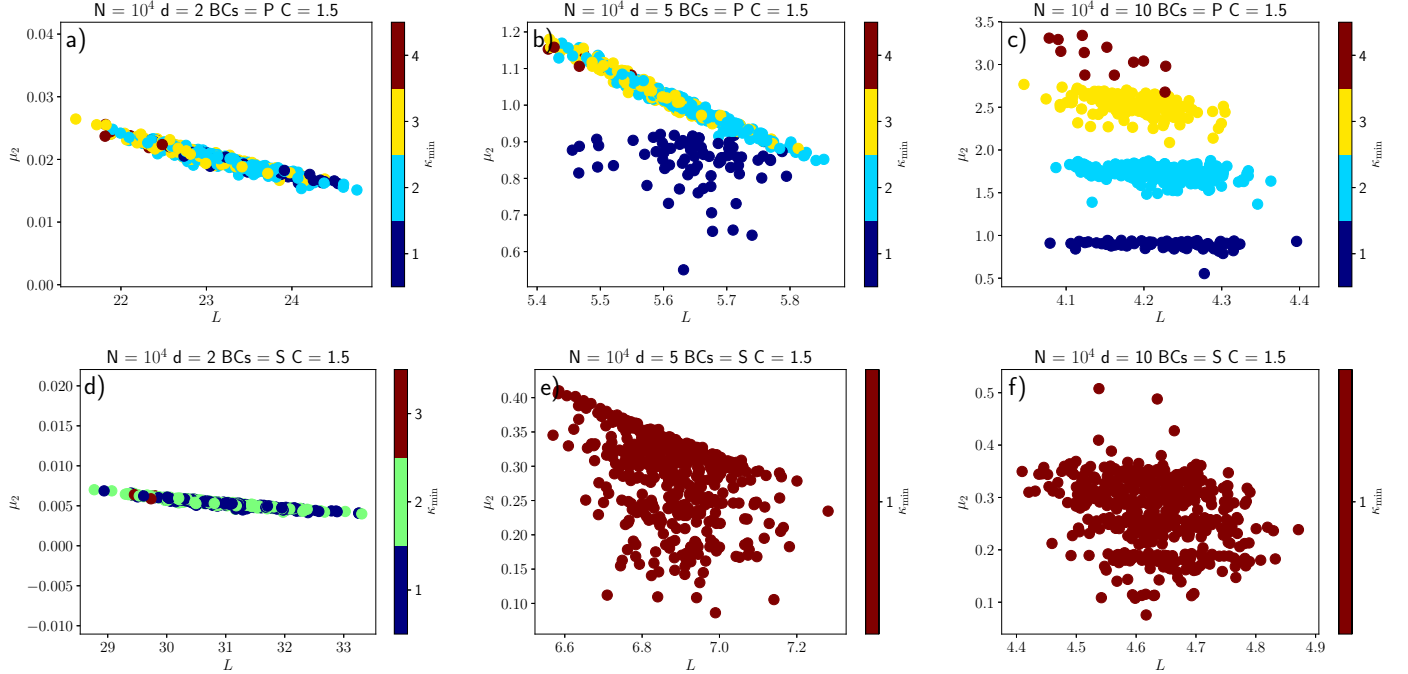


FIG. 4. **The modal structure of $\mathbb{P}(\mu_2)$ and structural correlates with μ_2 vary with the spatial dimension.** Scatter plot showing the joint distribution of μ_2 and L for different RGG ensembles with points coloured according to the corresponding value of κ_{\min} of each graph. As d is increased for fixed C the expected value of μ_2 increases, this is accompanied by a change in the form of $\mathbb{P}(\mu_2)$ from a single mode to a multimodal distribution. Shown for periodic (4a,4b and 4c) and solid (4d,4e and 4f) boundaries for RGG ensembles with $N = 10^4$ and $C = 1.5$. Each plot shows 500 draws from the corresponding ensemble.

C. Structural Factors Influencing $CV(\mu_2)$

In the preceding section we found that $CV(\mu_2)$, which measures the fluctuations in μ_2 relative to the ensemble mean, can become large in several regions of parameter space. We have identified four factors which can drive fluctuations in μ_2 for RGGs with uniform node distributions. We will treat these factors in isolation, however, it should be noted that there are some regions in parameter space where they can co-occur. These factors are:

Small System Size. We observe that $CV(\mu_2)$ increases as $N \rightarrow 0$. This coincides with large fluctuations in many other graphs properties due to the small system size. The presence of these fluctuations reflects the fact that smaller systems are inherently more noisy.

Connectivity Effects. As C is decreased for fixed N the mean degree of the corresponding RGG ensemble will also decrease. Figure 6 illustrates how the CV of μ_2 , L and N_{LCC} behave as the value of C is reduced below the connectivity threshold. All of the CVs increase significantly for values of C below 1, however, $CV(\mu_2)$ clearly begins to increase before this point. This indicates that the presence of more low degree nodes in the system can be important for driving fluctuations in μ_2 .

Figure 6b shows the behaviour of Spearman correlations $\rho(\mu_2, L)$ and $\rho(\mu_2, N_{LCC})$ behave as a function of C for $2d$ periodic RGGs. $\rho(\mu_2, L)$ is negative and large in magnitude. The most negative values of $\rho(\mu_2, L)$ co-

incide with the increase in $CV(L)$ in 6a indicating that large fluctuations in μ_2 coincide with those in L when C is small. $\rho(\mu_2, N_{LCC})$ is smaller in magnitude for larger values of C , however, it becomes significant for lower values of C where the size of the LCC in the RGG can fluctuate significantly.

Fluctuations in κ_{\min} . In section III A we observed that $\mu_2 \approx \kappa_{\min}$ in higher dimensional RGGs (Figure 4), which demonstrates that sample-to-sample fluctuations in κ_{\min} can drive those in μ_2 . Figure 7 shows $CV(\kappa_{\min})$ and $\rho(\mu_2, \kappa_{\min})$ as a function of N and C for the parameter range studied in 5.

For periodic RGGs (Figures 7a, 7b and 7c), $CV(\kappa_{\min})$ is largest when $C = 1.5$. This corresponds to the case when κ_{\min} only takes a few small values (for example we may have $\kappa_{\min} \in \{1, 2, 3\}$). In this case the fluctuations in κ_{\min} relative to its mean will be large. For $C = 1$ we observe that $CV(\kappa_{\min})$ is either small or zero. For this value of C either all or most of the sampled RGGs will have $\kappa_{\min} = 1$. For solid RGGs (Figures 7e, 7f and 7g) $CV(\kappa_{\min})$ is equal to zero for smaller values of C but is relatively large for large values of C . The former case corresponds to RGG ensembles where $\kappa_{\min} = 1$ for all graphs.

μ_2 and κ_{\min} become highly correlated for different parameter values in different RGG ensembles (Figures 7g-7l). The observed correlation is generally more significant for higher dimensional RGG ensembles, however, we also

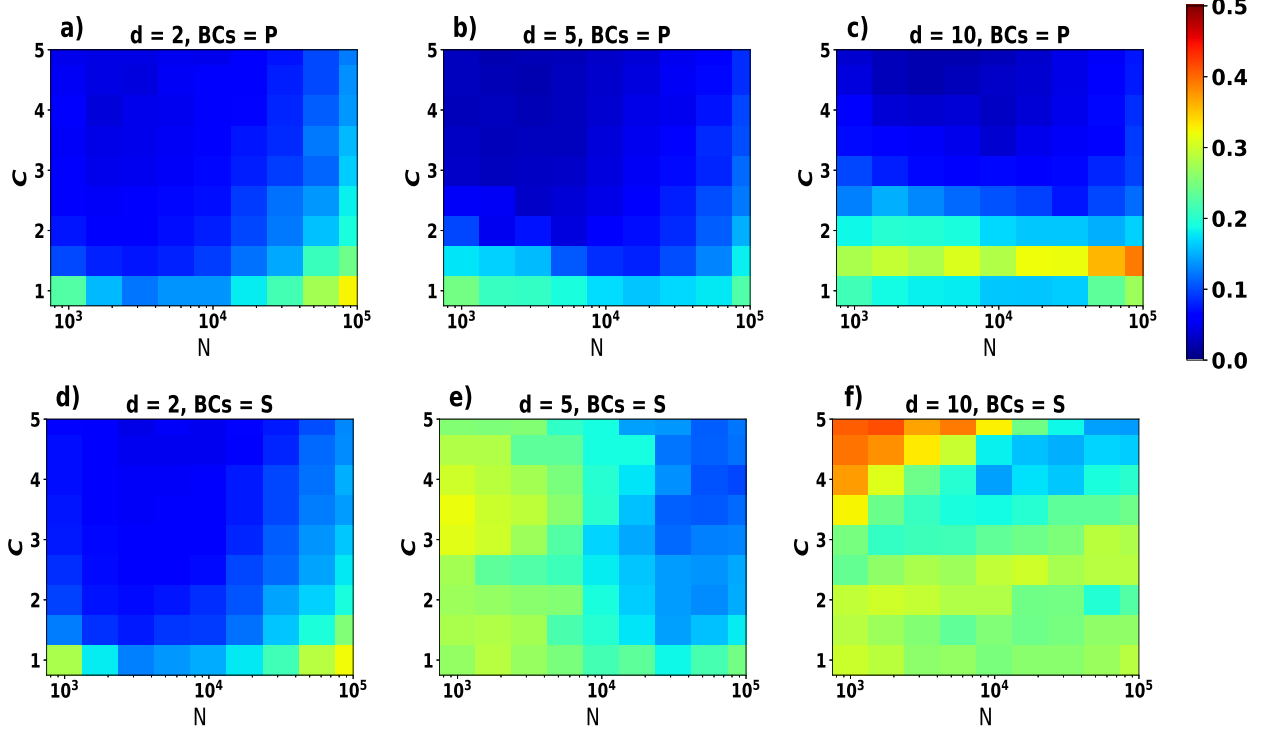


FIG. 5. $CV(\mu_2)$ can be large and vary non-monotonically with N . Heat plots showing how $CV(\mu_2)$ varies as a function of N and C for RGGs in $[0, 1]^d$ for different choices of d in both periodic and solid boundary conditions. Illustrates how changing N , C , d and the boundaries can all have an impact on the relative size of the sample-to-sample fluctuations in μ_2 in RGG ensembles. Values of $CV(\mu_2)$ above 0.3 are observed in all heat maps. This indicates that knowledge of $P(\underline{X})$ in these ensembles can only allow us to estimate μ_2 for a particular graph with a precision of approximately 30% of $\mathbb{E}(\mu_2)$. Each data point corresponds to 250 samples from the corresponding RGG ensemble.

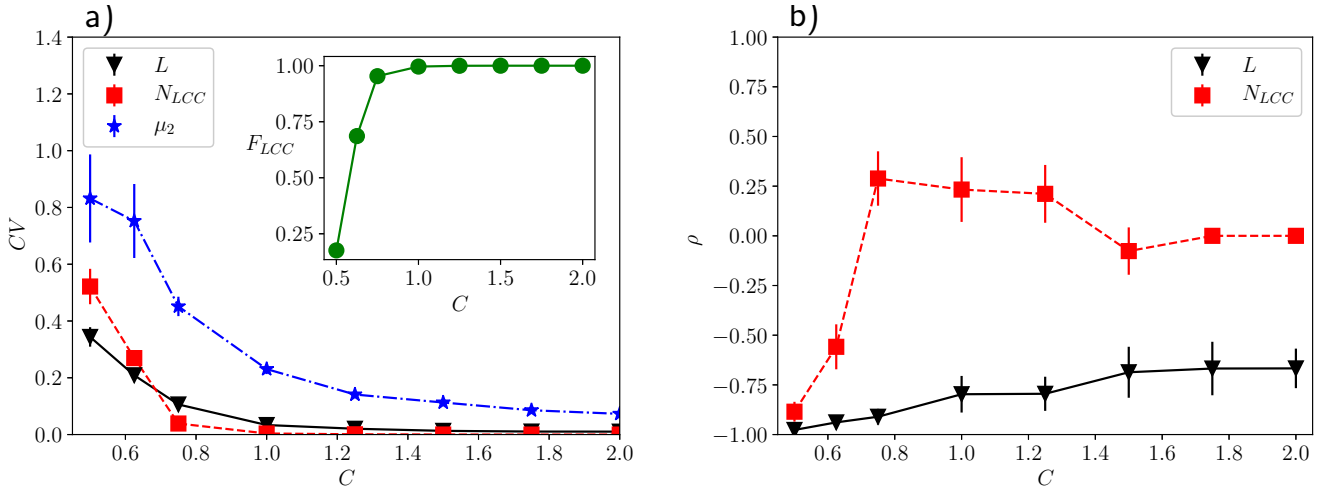


FIG. 6. Decreasing towards and going below the connectivity threshold causes large fluctuations in μ_2 . Plot showing how the CVs of graph properties vary as a function of the connectivity parameter, C for RGGs with periodic boundary conditions with $N = 10^3$. Figure 6a shows $CV(\mu_2)$, $CV(L)$ and $CV(N_{LCC})$ and 6b shows $\rho(\mu_2, L)$ and $\rho(\mu_2, N_{LCC})$. Also shown (inset) is the fraction of nodes in the LCC as a function of C . We note that the CV begins to rise before we reach the connectivity threshold at $C = 1$. Standard errors in the estimates of $CV(\mu_2)$ were computed using (A1) (see Appendix A). Error bars in ρ represent 95% confidence intervals obtained via bootstrapping. Each data point is computed from 100 samples from the corresponding RGG ensemble.

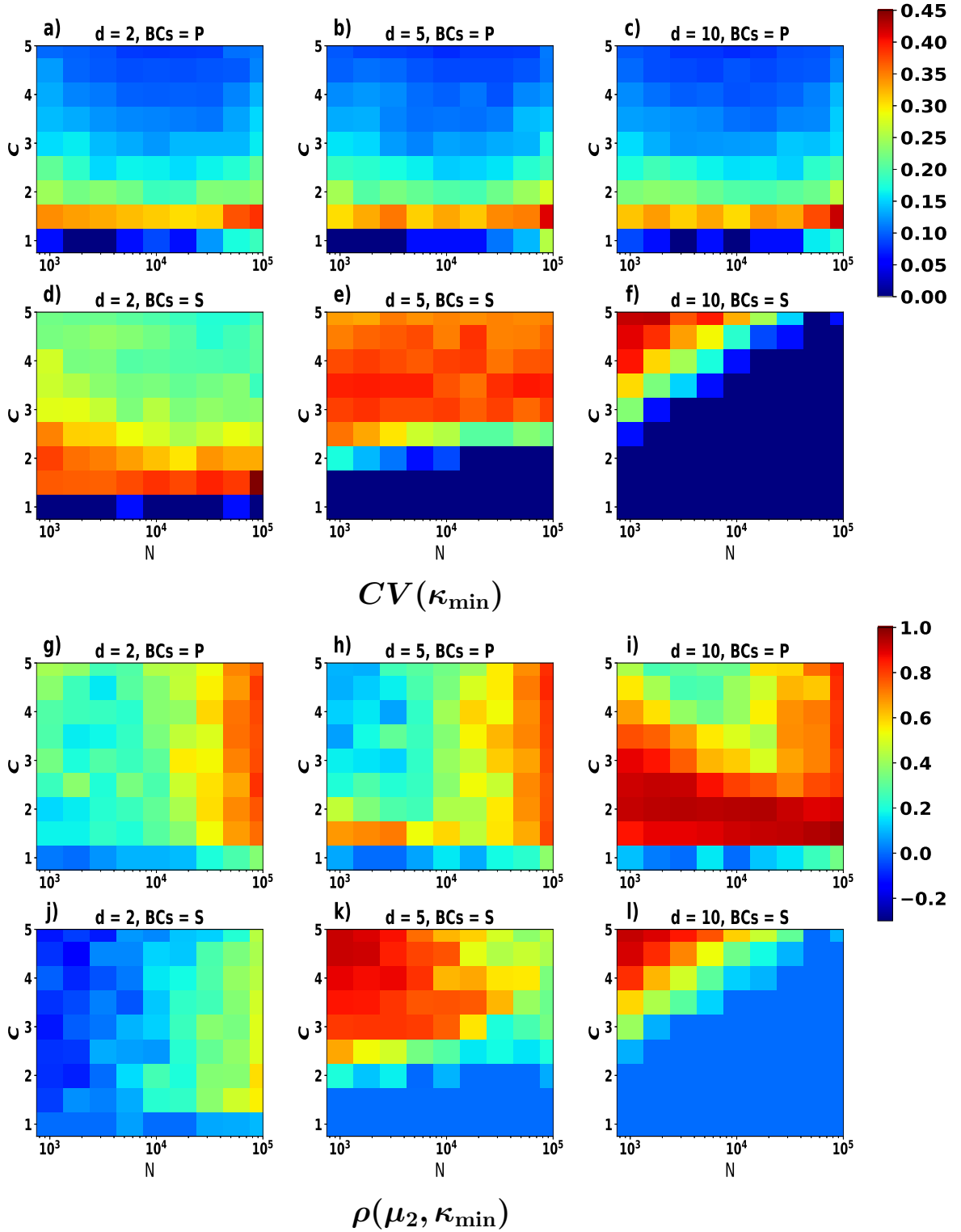


FIG. 7. **Large fluctuations in κ_{\min} can co-occur with those in μ_2 .** Plot showing $CV(\kappa_{\min})$ (7a-7f) and $\rho(\mu_2, \kappa_{\min})$ (7g-7l) as a function of N and C for the same parameter range as that in Figure 5. Large values of $CV(\kappa_{\min})$ are found for RGGs where the typical value of κ_{\min} is small. For periodic RGGs this occurs when $C > 1$ but not for $C \approx 1$ where the majority of RGGs drawn from the ensemble have $\kappa_{\min} = 1$. For solid RGGs the region in parameter space where $CV(\kappa_{\min}) \approx 0$ is much larger due to an increased probability of generating low degree nodes close to the boundary. The presence of these regions accounts for the non-monotonicity in $CV(\mu_2)$ observed previously (see 5c and 5f). $\rho(\mu_2, \kappa_{\min})$ is typically larger for higher dimensional systems, which is in agreement with our expectation that $\mu_2 \approx \kappa_{\min}$ for these graphs (see Section III A). However, we also observe an increase in the value of $\rho(\mu_2, \kappa_{\min})$ with N for the case of $d = 2$. Each data point corresponds to 250 samples from the corresponding RGG ensemble. Figures (7g-7l) are observed to be relatively noisy since some κ_{\min} values occur rarely meaning that $\rho(\mu_2, \kappa_{\min})$ cannot be estimated precisely.

observe an increase in $\rho(\mu_2, \kappa_{\min})$ as a function of N for the lower dimensional case. This latter result is not immediately intuitive as we expect the diffusion timescale in low dimensional RGGs to be dominated by spatial diffusion across the domain. In this case we would not expect the presence of a single weakly connected node to have a significant impact on the overall diffusion timescale. However, we can explain this effect in terms of density fluctuations (see the next remark).

Density Fluctuations in Large RGGs. For $2d$ RGGs we see an increase in $CV(\mu_2)$ with N . As shown above we find that $\rho(\mu_2, \kappa_{\min})$ increases with N . However, for RGG ensembles with $N \approx 10^5$ we find that $\rho(\mu_2, \kappa_{\min}) \lesssim 0.8$, which indicates that larger values of $CV(\mu_2)$ for large $2d$ RGGs cannot entirely be accounted for by large values of $CV(\kappa_{\min})$.

Two particular draws of \underline{X} from a uniform distribution of nodes may contain more or less highly clustered or dense regions. Since N is fixed, an excess of nodes in dense regions will in turn leave space for more sparse regions containing fewer nodes. Consequently, two particular draws of \underline{X} may be more or less inhomogeneous. The degree of this inhomogeneity will have an impact on the graph structure. For example, we might expect a graph containing more ‘holes’ to have a much longer typical timescale of diffusion and hence a smaller value of μ_2 .

We can quantify this effect on the corresponding RGG by considering the number of nodes with a particular degree K , which we denote by N_K . If N_K is larger than average for either small or large values of K then the corresponding node distribution will be more inhomogeneous. The total number of nodes in the graph is fixed so we will have $\sum_{K=1}^{\infty} N_K = N_{LCC}$. We can quantify the excess in (or deficit in) the number of nodes with low degree by considering:

$$\Sigma_{N_\kappa} = \frac{1}{N} \sum_{K=1}^{K=\lfloor \kappa \rfloor} N_K. \quad (10)$$

If Σ_{N_κ} is larger than its average value there will be an excess number of low-degree nodes in sparse regions of the domain, and also an excess of high degree nodes in dense clusters. The division by N in front of the summation allows us to keep track of the number of nodes with low degrees as a fraction of the total number of nodes.

For RGGs with uniform node distributions the degree distribution is asymptotically Poisson. Given this it is possible to derive the distribution of the N_K ’s. If P_K is the probability of drawing a node with degree K then the N_K ’s will be binomially distributed random variables with mean NP_K and standard deviation $\sigma_{N_K} = \sqrt{N(1-P_K)P_K}$. P_K will be the probability density of a Poisson distribution with parameter $\kappa = C \log(N)$. From this it is possible to find that:

$$CV(N_K) \approx \frac{\sqrt{K!} N^{\frac{C-1}{2}}}{(C \log(N))^{\frac{K}{2}}}, \quad (11)$$

for large N . This function diverges as $N \rightarrow \infty$ indicating that we expect fluctuations in N_K relative to their mean to increase.

Figures 8a and 8b show how $|\rho(\Sigma_{N_\kappa}, \mu_2)|$ and $CV(\Sigma_{N_\kappa})$ behave as a function of the system parameters for periodic RGGs in $[0, 1]^2$. $|\rho(\Sigma_{N_\kappa}, \mu_2)|$ increases from a value close to 0 to 1 as N is increased which demonstrates that inhomogeneities in the node density play an important role in determining the value of μ_2 in larger RGG ensembles. We also see a corresponding increase in $CV(\Sigma_{N_\kappa})$ as the system size is increased. This suggests that, for any two RGGs drawn from large RGG ensembles, the proportion of nodes with low degree can vary significantly. For example, for the ensemble with $N = 10^5$, $C = 2$ we observe that $\sigma(\Sigma_{N_\kappa}) \approx 0.12$ indicating that it is not unusual the number of nodes in the graph with degrees lower than κ can increase (or decrease) by 12% of N . The observed increase in $CV(\Sigma_{N_\kappa})$ is consistent with the prediction made for the fluctuations in individual N_K values in (11).

Relationship between Σ_{N_κ} and κ_{\min} . The density fluctuation effect offers a more intuitive explanation for the correlation between μ_2 and κ_{\min} observed in Figures 7h and 7l. For $2d$ RGGs find that $\mu_2 \ll \kappa_{\min}$ rather than $\mu_2 \approx \kappa_{\min}$ as in higher dimensional ensembles. However, graphs where the position set has a larger number of voids and clusters (ie. more inhomogeneity) are more likely to generate RGGs in which κ_{\min} itself is lower. Initial numerical results suggest that Σ_{N_κ} and κ_{\min} can be strongly correlated for RGG ensembles with $d = 2$ with large N , although, not necessarily for higher dimensional ensembles. However, a full discussion of this effect is beyond the scope of this work.

IV. NON-UNIFORM NODE DISTRIBUTIONS

A. Behaviour of $CV(\mu_2)$ in Gaussian RGGs

In the previous section we explored the factors which can drive fluctuations in μ_2 for ensembles of RGGs where the distribution of points is uniform. In this section we explore how non-uniformity in the node distribution can influence the statistical properties of μ_2 . We study the properties of $\mathbb{P}(\mu_2)$ for the ensemble of Gaussian RGGs in $d = 2$ (defined at the start of section III).

For uniform RGGs we have scaled the degree logarithmically in system size (ie. $\kappa = C \log(N)$) in order to tune the connectivity of the system. In RGGs with Gaussian node locations the degree distribution is non-Poissonian [2] and this choice will no longer allow us to achieve generate connected graphs. Consequently, we consider an increased range of C values for Gaussian RGGs and confirm the that $N_{LCC} \approx N$ by reporting the value of $F_{LCC} = \frac{N_{LCC}}{N}$.

Figure 9 illustrates how $CV(\mu_2)$ and F_{LCC} behave as a function of N and C for Gaussian RGGs. $CV(\mu_2)$ consistently takes values of 0.3 or above across the whole range

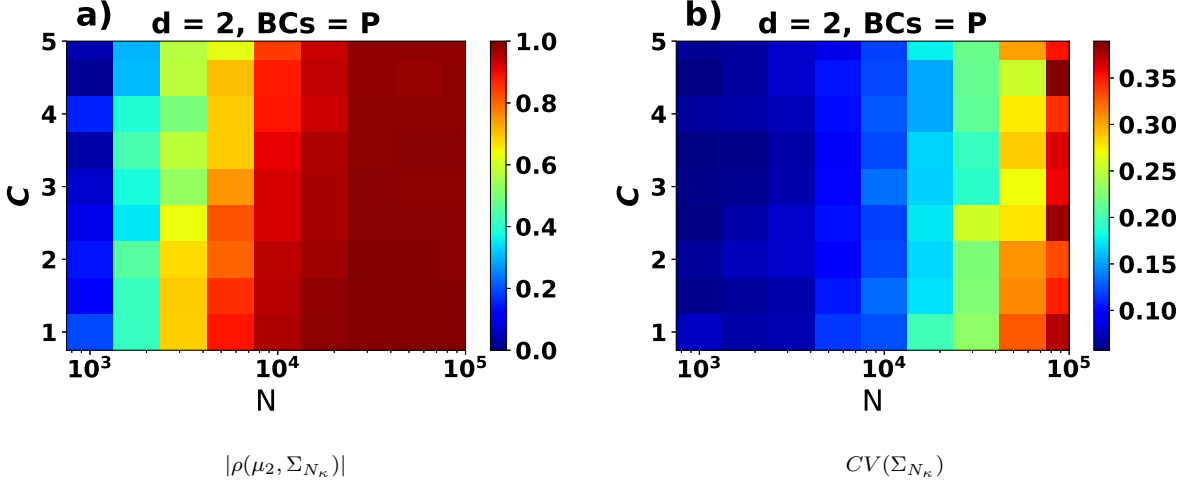


FIG. 8. **Fluctuations in the number of low density regions in \underline{X} can drive large fluctuations in μ_2 .** Heat plots showing how $|\rho(\mu_2, \Sigma_{N\kappa})|$ and $CV(\Sigma_{N\kappa})$ vary as a function of N and C for periodic RGGs with $d = 2$. Figure 8a illustrates how the correlation between $\Sigma_{N\kappa}$ and μ_2 increases in magnitude with N . Figure 8b shows how the sample-to-sample fluctuations in $\Sigma_{N\kappa}$ grow with N . Each data points corresponds to 250 samples from the corresponding RGG ensemble.

of parameters studied. This level of ensemble variability is more significant than that observed in $2d$ RGGs with uniform node distributions (Figures 5a and 5d). We also observe that $CV(\mu_2)$ decreases with N , which contrasts with the trend observed in the uniform case.

For smaller values of N the value of $CV(\mu_2)$ increases with C . In these ensembles it is possible to observe fluctuations in the value of κ_{\min} as it becomes possible to draw Gaussian RGGs with $\kappa_{\min} > 1$ for sufficiently large values of C . This demonstrates that fluctuations in κ_{\min} can also play a key role in driving those in μ_2 for non-uniform RGG ensembles with $d = 2$.

Figure 9b allows us to verify that a significant fraction ($> 90\%$) of the nodes lie in the LCC for the range of N and C values studied. The largest values of $CV(\mu_2)$ occur at large values of C where $F_{LCC} \approx 1$. This demonstrates that large values of $CV(\mu_2)$ cannot be attributed to significant variability in the LCC size.

In the previous section we explained the larger values of $CV(\mu_2)$ by considering the correlation of μ_2 and other graph metrics. For most of the parameter values studied the Gaussian RGGs sampled will have $\kappa_{\min} = 1$, which means that the variability in μ_2 cannot necessarily be explained by fluctuations in the minimum degree. We now demonstrate how large values of $CV(\mu_2)$ in Gaussian RGG ensembles can be explained by the presence of weakly connected subgraphs occurring in these graphs. The following section explores this in terms of the eigenvector corresponding to μ_2 .

B. Variability in the Fiedler Vector

In order to understand more about the factors which influence the algebraic connectivity in Gaussian RGG en-

sembles we study its corresponding eigenvector, \underline{u}_2 . This eigenvector is known as the *Fiedler vector* and has application in community detection algorithms [43]. Studying the components of \underline{u}_2 allows us to identify instances of tightly knitted communities in the network.

We denote the components of \underline{u}_2 as $(u_2^1, u_2^2, \dots, u_2^N)$. A simple heuristic for partitioning the nodes in the network into two groups is to split them according to the sign of the corresponding element of \underline{u}_2 [43], (also see [44] pg 89). That is, we assign node i to group 1 if $u_2^i \geq 0$ and otherwise we assign it to group 2.

We also note that for the graph Laplacian, the first eigenvector $\underline{u}_1 = (1, 1, \dots, 1)$ will be orthogonal to \underline{u}_2 . From this it follows that:

$$\sum_{i=1}^N u_2^i = 0. \quad (12)$$

Consequently, if a subset of the components of \underline{u}_2 are much larger in magnitude than the majority, then one of the two groups will be smaller in size. This indicates the presence of sub-community which is only weakly connected to the majority of the nodes.

We can keep track of the proportion of nodes assigned to each partition. If we let N_1 and N_2 be the number of nodes assigned to groups 1 and 2 respectively then we can define:

$$F_P = \frac{\min(N_1, N_2)}{N_{LCC}}. \quad (13)$$

This quantity keeps track of the fraction of nodes assigned to the smaller group. Given that $\sum_i u_i = 0$ a smaller value of F_P will also imply localisation of a large amount of mass of the eigenvector onto a smaller number of nodes. We also consider the magnitude of the largest

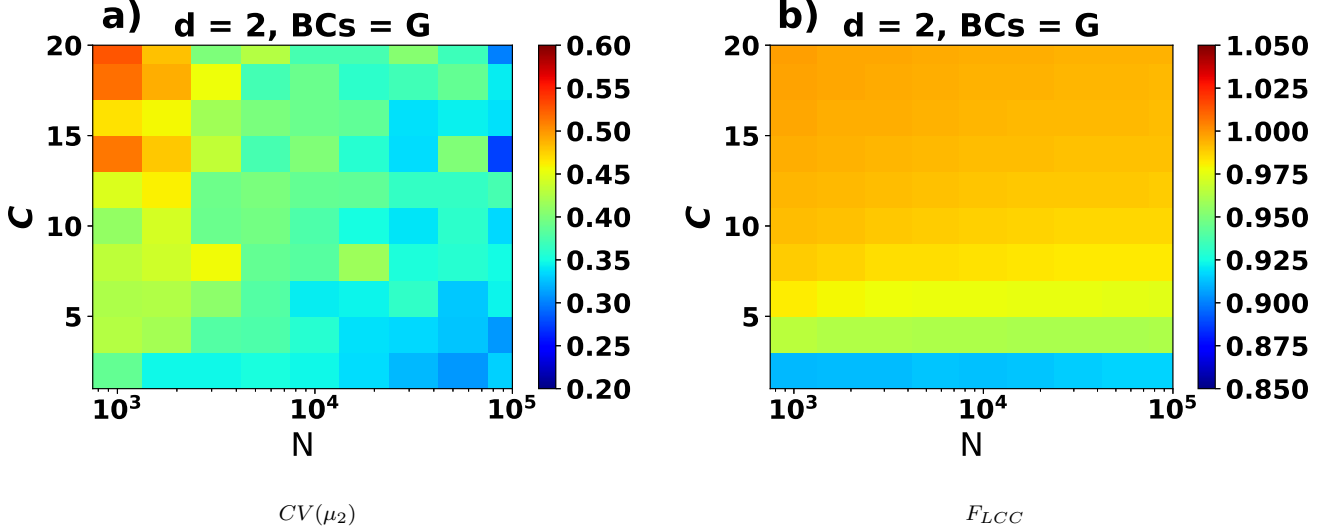


FIG. 9. $CV(\mu_2)$ is large in Gaussian RGG ensembles for a wide range of mean degrees and system sizes. Heat plots showing $CV(\mu_2)$ and F_{LCC} as a function of N and C for RGGs with Gaussian node positions. The values of $CV(\mu_2)$ observed are equal to and greater than some of the largest values for RGGs with uniform node positions in Figure 5. Figure 9b demonstrates that the average size of the LCC does vary dramatically for the range of N and C values considered. Each pixel corresponds to 200 samples for the ensemble for $N < 5 \times 10^4$ and 90 samples otherwise.

component in the Fiedler vector $u_2^{\max} = \max_i(|u_2^i|)$. This quantity is informative about the single node which has the largest amount of mass of the eigenvector.

Figure 10a shows F_P plotted against $\frac{\mu_2}{\mathbb{E}(\mu_2)}$ for different RGG ensembles (where the division by $\mathbb{E}(\mu_2)$ is performed so we can plot ensembles with different means on the same axis). In Gaussian RGGs the value of F_P is small indicating that the smaller partition is a relatively small subgraph of the network. F_P also shows some co-variation with μ_2 which suggests that small weakly connected subgraphs appear with an appreciable frequency but are not guaranteed. In uniform RGGs with $d = 2$, $F_P \approx 0.5$ for all graphs drawn from the ensemble. In contrast, for $d = 10$, F_P shows variability between 0.2 and 0.5 indicating that the size of the suggested partition fluctuates considerably.

Figure 10b shows how u_2^{\max} varies for different RGG ensembles. For $d = 2$ we find that $u_2^{\max} \sim O(\frac{1}{N})$ indicating that the mass of the Fiedler vector is spread out across the nodes. In contrast, for the case of $d = 10$, where κ_{\min} is important for determining μ_2 , we see that the value of u_2^{\max} can fluctuate between values close to zero and close to one. Comparing Figure 10b with 4c shows that the nodes in $\mathbb{P}(\mu_2)$ corresponding to $\kappa_{\min} = 1, 2, 3$ correspond to the eigenvector being highly localised onto a single node, while the node corresponding to $\kappa_{\min} = 4$ has a significantly smaller value of u_2^{\max} suggesting that the components of the eigenvector are spread out across the graph. For Gaussian RGGs u_2^{\max} takes an intermediate value indicating that a single node can possess a large amount of the total mass of the eigenvector.

Figures 10c, 10d and 10e show three draws from the

ensemble of GRGGs with low, medium and high values of μ_2 for the corresponding ensemble. When μ_2 is relatively large we observe that the corresponding partition is almost even (Figure 10e), whereas, when μ_2 is small, the elements of \underline{u}_2 corresponding to the second partition are localised onto a small weakly connected subgraph (Figure 10c).

It is worth noting here that the degree to which the eigenvector concentrates on a single node (or group of nodes) can also be quantified using measures such as the *Inverse Partitioning Ratio* [45] or the *localisation length* [34]. However, for the case of the current study we believe the information contained in F_P and u_2^{\max} are sufficient to illustrate the range of factors influencing μ_2 in the different classes of RGG ensemble.

V. DISCUSSION

A. Ensemble Variability in RGGs

Node attributes and metadata such as geographic coordinates are often informative about the structure of complex networks. Gaining access to this data may be easier than obtaining the full graph structure, which may also be unnecessary if the aim is only to predict bulk properties of the graph. The aim of this study was to investigate the degree to which knowledge of node locations in RGGs gives an advantage over only having access to the distribution of node locations.

The question posed above can be rephrased as one about whether properties of RGGs are “ensemble averageable”. In this study we have focused on the ensemble

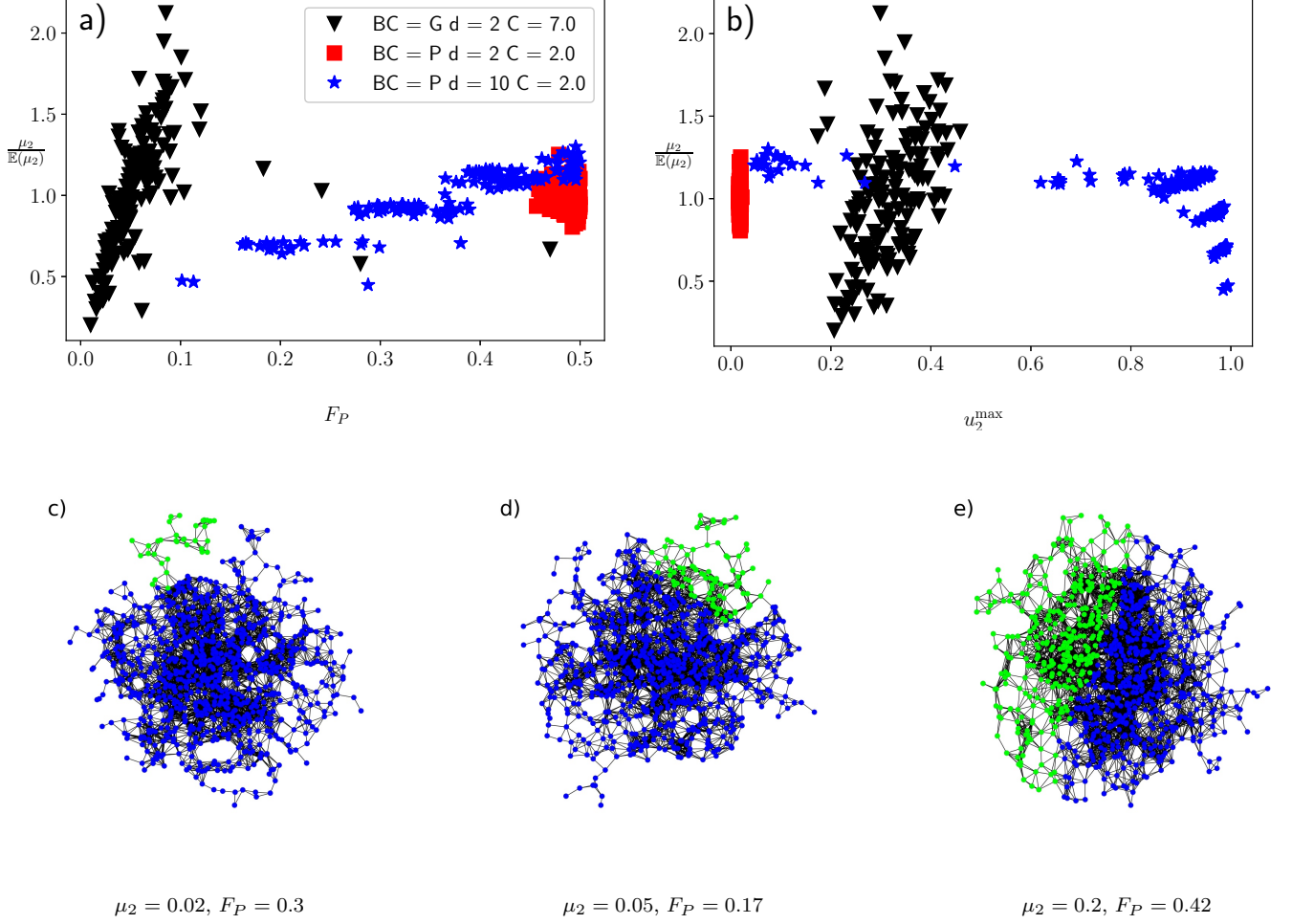


FIG. 10. **Different classes of eigenvector localisation can drive Fluctuations in μ_2 .** Plots illustrating the effect of eigenvector localisation on μ_2 . Figures 10a and 10b show $\mu_2/\mathbb{E}(\mu_2)$ as a function of F_P , the fraction of nodes in the smaller Fiedler partition and u_2^{\max} for three different RGG ensembles with $N = 10^4$. Shown for Gaussian RGGs with $C = 7, d = 2$ (black triangles) and periodic RGGs with $C = 2$ for $d = 2$ and $d = 10$ (red squares and blue stars). In each case we take 150 samples from the ensemble. Figures 10c, 10d and 10e show graphs drawn from the ensemble of Gaussian RGGs with $N = 10^3, d = 2$ and $\kappa = 20.0$. Showing graphs with the minimum, median and maximum μ_2 values from 101 draws from an ensemble with $\mathbb{E}(\mu_2) = 0.06$. Nodes are coloured according the sign of the corresponding element of the Fiedler vector, \underline{u}_2 . This illustrates how the number of nodes in the Fiedler partition can be highly variable.

variability of μ_2 since it is of interest when studying the dynamical properties of networks. We have quantified the sample-to-sample variability in μ_2 by estimating the coefficient of variation of its distribution. This metric provides a measure of how robustly we can estimate μ_2 for a random draw from the ensemble given knowledge of $P(\underline{X})$ and R . In some applications an order of magnitude estimate of the quantity of interest may be sufficient, however, for cases where we wish to estimate a quantity precisely, fluctuations greater than 5 – 10% of the size of the mean value may be considered significant.

Our results indicate that $CV(\mu_2)$ can exceed values of 0.3 in ensembles with 10^5 nodes for a range of choices of dimension and boundary condition (Figure 5). The presence of a relatively large values of $CV(\mu_2)$ for rel-

atively large graphs demonstrates that RGG ensembles exist where μ_2 is not well represented by the ensemble mean. This finding contrasts with those in [21] where they found that the extremal eigenvalues of the Laplacian for certain scale-free networks are typically ensemble averageable. We also find that $CV(\mu_2)$ is large in ensembles where κ_{\min} is small, and that κ_{\min} can play an important role in driving the fluctuations in μ_2 . This is consistent with the findings in [22] where they find that large fluctuations in μ_2 are generally observed in networks with low minimum degrees.

The presence of *multimodality* in the μ_2 distributions of RGGs (Figure 4c) demonstrates that the behaviour observed in [22] was not just an artefact of the real world network ensembles studied and also occurs in well stud-

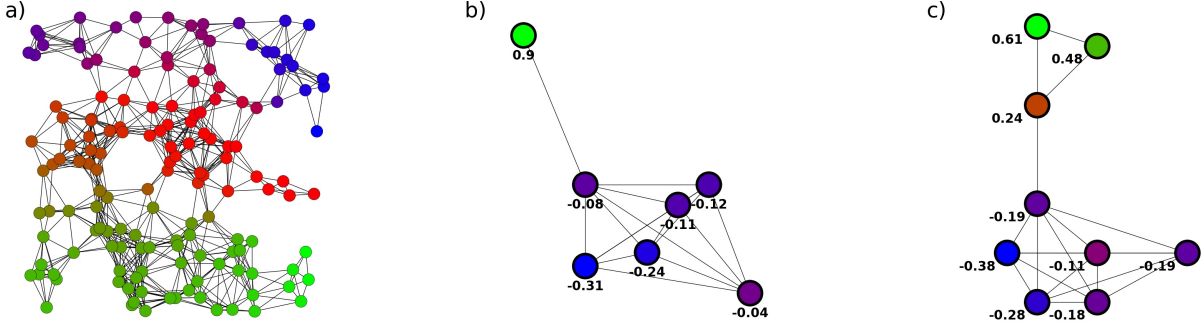


FIG. 11. **Schematic illustrating the different divisions of Fiedler vector components which can occur in the RGG ensembles studied.** 11a Shows the case when the partition is approximately even. In this case μ_2 can be influenced by statistical properties of the network such as the mean shortest path length, L . This regime is found in solid and periodic RGGs with $d = 2$. 11b Shows the case where most of the mass of the eigenvector is localised onto a single low degree node. In this case the value of μ_2 can be strongly correlated with κ_{\min} . This regime is found in ER graphs as well as solid and periodic RGGs in higher dimensions. 11c Shows that case where the much of the mass of the eigenvector is concentrated onto a weakly connected subgraph. This case is observed in Gaussian RGGs. In both 11b and 11c we can see large fluctuations in μ_2 across the ensemble as the presence of weakly-connected subgraph or low degree node is a chance event which occurs with an appreciable frequency. In cases b) and c) the values of Fiedler vector components corresponding to each node are shown.

ied random graph models. This multimodality was found to arise due to the strong correlation between μ_2 and κ_{\min} . In [22] they hypothesize that the main factors likely to drive large fluctuations in μ_2 across the ensemble are the presence of low degree nodes, the presence of ‘bottleneck’-like subgraphs and communities of densely connected nodes which are sparsely connected to the rest of the network. We conjecture that the latter factors may be the causes of the multiple modes observed in $\mathbb{P}(\mu_2)$ for graphs which all have the same value of κ_{\min} (Figures 4e and 4f).

One could interpret the results presented as evidence that μ_2 is not necessarily the best metric to rely on when attempting to describe the bulk dynamical properties of the network; especially because it can be sensitive to microscopic properties of the network (ie. κ_{\min}) in certain ensembles. Recent work in [46] compared RGGs generated from uniform random distributions with those where the positions are generated from ‘quasi-random’ sequences. They found that the assortativity, spectral gap and μ_2 were most strongly effected by the change in the nodal distribution. This observation was explained by noting that ‘quasi-random’ point distributions generally appear more uniform leading to fewer clusters and holes in the RGG. This supports our hypothesis that the presence of non-uniformity or regions of low density in the node distribution can lead to significant fluctuations in the value of μ_2 .

Eigenvector Localisation. It is also possible to interpret the results in terms of the localisation properties

of the Fiedler vector. We can identify three notable cases of how the eigenvector can behave in the network ensembles studied (Figure 11). Firstly, a roughly even division of the positive and negative values of the Fiedler vector components between the nodes (Figure 11a). Secondly, concentration of most of the eigenvectors mass onto a single node (Figure 11b). Finally, splitting of positive and negative components either side of a bottleneck (Figure 11c).

The presence of localisation of the eigenvector demonstrates that the value of μ_2 for a particular network can be influenced strongly by the edges incident to some small subset of nodes in the graph. This phenomena is discussed in [47] where they conclude that this implies that the bulk statistical properties of a network are unlikely to be predictive of μ_2 . We have shown that this appears to be the case for higher dimensional RGGs with uniform node distributions where the presence of a single node with a lower degree can dramatically influence the value of μ_2 (Figure 4c). We also see that this can also occur in Gaussian RGGs (Figure 10) where the presence of a small weakly connected subgraph can lower the value of μ_2 significantly.

An alternative conclusion is presented in [48]. They note that the above can be true in some graph ensembles, however, there are certain cases where macroscopic statistical properties of graphs can determine their spectral properties. They show that the synchronisation index (which is a function of the Laplacian eigenvalues) can be correlated with bulk statistical properties in some

random graph ensembles. Our results are more in accordance with this for uniform RGGs with $d = 2$ where μ_2 can become correlated with bulk statistical properties such as L (Figure 6b) and Σ_{NK} , which describes the inhomogeneity in \underline{X} (Figure 8a).

B. Implications for Node Location Knowledge in Geometric Networks

Based on the argument made in IA (in particular see Figure 2) we expect knowledge of node locations in the embedding space to be of utility when $CV(\mu_2)$ is large. Precise knowledge of node locations may be possible in engineered systems such as wireless communications networks, whereas, in many other systems, such as large scale social networks, data may be noisy or inaccurate. We find that $CV(\mu_2)$ can be large for several different reasons. In each case there are different implications for the utility of node location knowledge:

1. For RGG ensembles with uniform node distributions close to and below the connectivity threshold fluctuations in μ_2 appear to be associated with fluctuations in L , and N_{LCC} (Figure 6b). This suggests that we require relatively precise knowledge of the node locations and that knowledge of node locations in low-density regions may be of most utility as these may allow us to identify whether the graph is connected.
2. In higher dimensional RGGs with uniform node distributions μ_2 can be determined by the presence of a single weakly connected node. In this case we may require detailed knowledge of both X_i 's for all nodes and R to obtain a precise estimation of μ_2 .
3. For larger RGGs with $d = 2$, chance inhomogeneities in the node distribution can have a significant effect on μ_2 . In this case knowledge of the node locations may be of utility.
4. For Gaussian RGGs we have evidence that the presence of mesoscopic subgraphs drive changes in μ_2 (Figure 10). This suggests that μ_2 now depends on mesoscopic variation in the graph structure rather than microscopic fluctuations. This implies that knowledge of node locations may yield some predictive power, even in the case where this knowledge is not precise.

It is worth noting that for RGGs with uniform nodes distributions with solid boundaries and Gaussian node positions, the fluctuations in μ_2 are driven by events occurring at the boundary of the domain (or edge of the support of the Gaussian). This suggests that, when it comes to predicting μ_2 and related metrics that *knowledge of node locations at the boundary will be of most utility*.

For uniform node distributions in low dimensions with large κ values the value of $CV(\mu_2)$ is relatively small (Figure 5). This suggests that knowledge of network properties such as μ_2 for a particular graph might be obtained

with a reasonable precision simply by sampling from an ensemble with an equivalent node distribution and connection radius. In this case, additional knowledge of \underline{X} over $P(\underline{X})$ may not be of significant utility. In [49] they use graph entropy in order to quantify the predictive advantage gained from knowledge of \underline{X} in $2d$ Soft RGGs. They find that knowledge of node locations can account for the vast majority of network structure. In this work we have shown that, even when knowledge of \underline{X} gives us full knowledge of the graph structure (as in the RGGs), structural and dynamically relevant properties may vary little between different graphs drawn from the same ensemble.

C. Future Prospects

In this work we have characterised ensemble variability in RGGs in terms of the variability in μ_2 . A complementary approach to quantifying the degree of variability or ‘topological uncertainty’ in a random graph ensemble is through the notion of graph entropy. This has recently been studied in RGGs [50–52]. An interesting avenue of future research will be to explore the degree to which topological uncertainty in the graph structure (as measured by entropy or other metrics) coincides with large variability in the dynamical properties. Furthermore, in Soft RGGs we can also consider entropies which are conditioned on the internode distances [51] or node locations [53]. Studying these along with the level of ensemble variability in graph properties would allow us to understand how informative node locations are in graphs with probabilistic connection functions.

The adjacency and Laplacian matrices of RGGs and Soft RGGs take the form of Euclidean Random Matrices (ERMs) in which matrix entries are functions of the random positions. Results exist for the expected values of their eigenvalues in the asymptotic limit [54] and it has also been shown that the spectra of these matrices have certain properties in common with well studied ensembles from Random Matrix Theory [33]. However, to the authors knowledge, no analytic results exist concerning the distributional properties of individual eigenvalues in these systems. We have shown that these distributions can behave in a non-trivial manner in response to changes in the system parameters (Figure 4). Consequently, we believe that it is of interest to obtain a theoretical understanding of the factors leading this. For example, it would be of interest to extend theoretical techniques in order to find an expression for $CV(\mu_2)$ and if possible provide a full characterization of $\mathbb{P}(\mu_2)$.

A wide range of real world systems can be modelled with ensembles of RGGs and their generalizations [1, 2, 6–8, 11–13]. These consist of both spatially embedded systems and graphs where the nodes possess other attributes which are relevant to tie formation. Providing limits on how much we can predict about the properties of these graphs given the available data is essential

for quantifying uncertainty in results and understanding level of data required for a specific application. This study takes the first step in this direction by attempting to understand the factors which drive variability in dynamically relevant properties of RGGs. Our results suggest that the amount we can predict about a graph given node locations or a distribution can vary significantly for different RGG ensembles. This suggests that knowledge of the generative process that leads to the formation of a network or detailed knowledge of the relevant node attributes and their corresponding distributions may be required when attempting to estimate graph properties without full access to the graph structure.

ACKNOWLEDGEMENTS

This work has been supported by EPSRC grants EP/L016613/1 (Centre for Doctoral Training in the

Mathematics of Planet Earth) and EP/N014529/1 (Centre for the Mathematics of Precision Healthcare). The authors thank Till Hoffman and Spencer Wilson for their contributions to the code base and useful discussions. Thanks to Thomas Gibson and Carl Dettmann for their comments on the manuscript. Simulations were performed using Imperial College High Performance Computing cluster: Imperial College Research Computing Service, DOI: [10.14469/hpc/2232](https://doi.org/10.14469/hpc/2232).

-
- [1] M. Barthélemy, *Phys. Rep.* **499**, 1 (2011).
 - [2] L. Barnett, E. Di Paolo, and S. Bullock, *Phys. Rev. E* **76**, 056115 (2007).
 - [3] M. Penrose, *The Annals of Applied Probability* **26**, 986 (2016).
 - [4] C. P. Dettmann and O. Georgiou, *Phys. Rev. E* **93**, 032313 (2016).
 - [5] A. P. Giles, O. Georgiou, and C. P. Dettmann, *J. Stat. Phys.* **162**, 1068 (2016).
 - [6] C. T. Butts and R. M. Acton, *The Sage Handbook of GIS and Society Research*. Thousand Oaks, CA: SAGE Publications, 222 (2011).
 - [7] C. T. Butts, R. M. Acton, and C. S. Marcum, *Journal of Social Structure* **13** (2012).
 - [8] G. Daraganova, P. Pattison, J. Koskinen, B. Mitchell, A. Bill, M. Watts, and S. Baum, *Soc. Networks* **34**, 6 (2012).
 - [9] I. Glauche, W. Krause, R. Sollacher, and M. Greiner, *Physica A* **325**, 577 (2003).
 - [10] H. Kenniche and V. Ravelomananana, in *Computer and Automation Engineering (ICCAE), 2010 The 2nd International Conference on*, Vol. 4 (IEEE, 2010) pp. 103–107.
 - [11] R. O’Dea, J. J. Crofts, and M. Kaiser, *J. R. Soc. Interface* **10**, 20130016 (2013).
 - [12] Y. P. Lo, R. ODea, J. J. Crofts, C. E. Han, and M. Kaiser, *Scientific reports* **5**, 15397 (2015).
 - [13] J. Hackl and B. T. Adey, in *14th International Probabilistic Workshop* (Springer, 2017) pp. 217–230.
 - [14] Y. Leo, E. Fleury, J. I. Alvarez-Hamelin, C. Sarraute, and M. Karsai, *J R Soc Interface* **13**, 20160598 (2016).
 - [15] J. R. Hipp, C. T. Butts, R. Acton, N. N. Nagle, and A. Boessen, *Soc Networks* **35**, 614 (2013).
 - [16] C. T. Butts, R. M. Acton, J. R. Hipp, and N. N. Nagle, *Soc. Networks* **34**, 82 (2012).
 - [17] P. D. Hoff, A. E. Raftery, and M. S. Handcock, *J Am Stat Assoc* **97**, 1090 (2002).
 - [18] D. Krioukov, F. Papadopoulos, M. Kitsak, A. Vahdat, and M. Boguñá, *Phys. Rev. E* **82**, 036106 (2010).
 - [19] F. Papadopoulos, M. Kitsak, M. Á. Serrano, M. Boguñá, and D. Krioukov, *Nature* **489**, 537 (2012).
 - [20] K.-K. Kleineberg, M. Boguñá, M. Á. Serrano, and F. Papadopoulos, *Nat Phys* **12**, 1076 (2016).
 - [21] D.-H. Kim and A. E. Motter, *Phys. Rev. Lett.* **98**, 248701 (2007).
 - [22] N. Carlson, D.-H. Kim, and A. E. Motter, *Chaos* **21**, 025105 (2011).
 - [23] M. E. J. Newman, *Networks: an introduction* (OUP, 2010).
 - [24] E. Estrada and G. Chen, *Chaos* **25**, 083107 (2015).
 - [25] F. Dörfler, M. Chertkov, and F. Bullo, *P. Natl. Acad. Sci. USA* **110**, 2005 (2013).
 - [26] L. Donetti, F. Neri, and M. A. Muñoz, *J. Stat. Mech.-Theory. E* **2006**, P08007 (2006).
 - [27] S. Barbarossa, G. Scutari, and A. Swami, in *Acoustics, Speech and Signal Processing, 2007. ICASSP 2007. IEEE International Conference on*, Vol. 2 (IEEE, 2007) pp. II–841.
 - [28] S. Sardellitti, S. Barbarossa, and A. Swami, *IEEE Transactions on Signal Processing* **60**, 383 (2012).
 - [29] R. Olfati-Saber, in *American Control Conference, 2005. Proceedings of the 2005* (IEEE, 2005) pp. 2371–2378.
 - [30] E. Estrada and M. Sheerin, *Physica D* **323**, 20 (2016).
 - [31] A. Bonato, D. F. Gleich, M. Kim, D. Mitsche, P. Pralat, Y. Tian, and S. J. Young, *PloS One* **9**, e106052 (2014).
 - [32] T. P. Peixoto, *Phys. Rev. Lett.* **111**, 098701 (2013).
 - [33] C. P. Dettmann, O. Georgiou, and G. Knight, *Europhys. Lett.* **118**, 18003 (2017).
 - [34] L. Alonso, J. A. Méndez-Bermúdez, A. González-Meléndrez, and Y. Moreno, *Journal of Complex Networks* (2017).
 - [35] C. P. Dettmann and G. Knight, *Journal of Complex Networks* (2017).
 - [36] A. Jamakovic and P. Van Mieghem, in *International Conference on Research in Networking* (Springer, 2008) pp. 183–194.
 - [37] J. P. Coon, C. P. Dettmann, and O. Georgiou, *J. Stat. Phys.* **147**, 758 (2012).

- [38] J. F. Donges, Y. Zou, N. Marwan, and J. Kurths, *Europhys. Lett.* **87**, 48007 (2009).
- [39] M. Penrose, *Random geometric graphs*, 5 (OUP, 2003) p. 10.
- [40] For details see <https://docs.scipy.org/doc/scipy-0.18.1/reference/tutorial/arpack.html>.
- [41] R. Rastelli, N. Friel, and A. E. Raftery, *Network Science* **4**, 407 (2016).
- [42] J. Dall and M. Christensen, *Phys. Rev. E* **66**, 016121 (2002).
- [43] M. E. J. Newman, *Phys. Rev. E* **74**, 036104 (2006).
- [44] P. Van Mieghem, *Graph spectra for complex networks* (Cambridge University Press, 2010).
- [45] R. Pastor-Satorras and C. Castellano, *Sci. Rep-UK* **6** (2016).
- [46] E. Estrada, *Phys. Rev. E* **96**, 022314 (2017).
- [47] F. M. Atay, T. Bıykoğlu, and J. Jost, *Physica D* **224**, 35 (2006).
- [48] S. Cardanobile, V. Pernice, M. Deger, and S. Rotter, *PLoS one* **7**, e37911 (2012).
- [49] C. T. Butts, *Predictability of large-scale spatially embedded networks* (National Academies Press, Washington, 2003).
- [50] J. P. Coon, in *Global Communications Conference (GLOBECOM), 2016 IEEE* (IEEE, 2016) pp. 1–6.
- [51] J. P. Coon, C. P. Dettmann, and O. Georgiou, *Phys. Rev. E* **97**, 042319 (2018).
- [52] M. A. Badiu and J. P. Coon, *arXiv preprint arXiv:1801.04757* (2018).
- [53] A. Hala, S. Mukherjee, and G. Bianconi, *Phys. Rev. E* **89**, 012806 (2014).
- [54] C. Bordenave, *Random. Struct. Algor.* **33**, 515 (2008).
- [55] P. Wonnapijit, P. F. Chinnery, and D. C. Samuels, *Am. J. Hum. Genet.* **86**, 540 (2010).
- [56] M. Abramowitz and I. A. Stegun, *Handbook of mathematical functions: with formulas, graphs, and mathematical tables*, Vol. 55 (Courier Corporation, 1964).

APPENDIX

Appendix A: Standard Error in the Coefficient of Variation

In order to estimate the statistical uncertainty in the CV we require an estimate for the standard error in the variance of a sample. For a sample $\underline{y} = (y_1, y_2, \dots, y_N)$ with mean $\langle y \rangle$, the standard error on the variance of the sample is given by: [55]

$$\sigma_{SE}(Var) = \sqrt{\frac{1}{N} \left(D_4 - \frac{N-3}{N-1} \sigma^4 \right)}, \quad (A1)$$

where D_4 is the fourth central moment of the sample. An unbiased estimator for this quantity can be calculated from:

$$D_4 = \frac{(N-1)}{N^3} \left((N^2 - 3N + 3)M_4 + 3(2N-3)M_2^2 \right), \quad (A2)$$

where:

$$M_j = \frac{1}{N} \sum_{i=1}^N (y_i - \langle y \rangle)^j. \quad (A3)$$

Combining (A1) this with the standard error in the mean using traditional error propagation techniques to obtain an estimate for the uncertainty on the coefficient of variation. The results obtained using (A1) were validated by comparison with an estimate of the standard error computed via a standard bootstrapping method.

Appendix B: Analytic Formula for the Algebraic Connectivity

In this section we present an analytic formula to approximate the average algebraic connectivity for RGGs with periodic boundaries in $[0, 1]^d$. The formula derived applies for RGGs with uniform node distributions, however, the techniques used could also be applied to both the non-uniform node distributions and networks with soft connection functions.

1. Derivation

In order to derive an analytic expression for μ_2 we consider the more general case of Soft Random Geometric Graphs [4]. For these graphs connections between nodes are now made probabilistically given the node positions. A connection between nodes at positions \underline{x}_i and \underline{x}_j is made with probability $\gamma(|\underline{r}|)$, where $\underline{r} = \underline{x}_i - \underline{x}_j$. We will refer to this function as the connection function.

The adjacency matrix of a Soft RGG takes the form of a Euclidean Random Matrix (ERM). An ERM, M , is a matrix where the entries are functions of positions in Euclidean space. This means that the entries take the form:

$$M_{ij} = F(|\underline{x}_i - \underline{x}_j|), \quad (B1)$$

where F is some measurable mapping and \underline{x}_i are positions in some domain. In [54] it is shown that the eigenvalues of an ERM can be expressed in terms of the Fourier coefficients of the connection function. In particular, the eigenvalues of the adjacency matrix of a spatial network with a uniform distribution of points on the unit torus take the form:

$$\lambda_i = N \hat{\gamma}(\underline{k}), \quad (B2)$$

where $\hat{\gamma}(\underline{k})$ are the Fourier coefficients of the connection function. These can be expressed as:

$$\hat{\gamma}(\underline{k}) = \int_{\mathbb{R}^n} \gamma(\underline{r}) e^{-2\pi i \underline{k} \cdot \underline{x}} d\underline{x}, \quad (B3)$$

where $\underline{k} \in \mathbb{Z}^d$. We note here that for a non-uniform distribution of positions the integration with respect to

$d\mathbf{r}$ can be replaced by an integration with respect to the probability measure of interest.

In [28] these results are applied to derive an expression for the algebraic connectivity of an RGG with points in a two dimensional periodic domain. We now generalize this result to the case of an RGG in a d dimensional periodic domain.

In order to determine the second smallest eigenvalue of L we note that the eigenvalues of the matrix with entries $\delta_{ij}K_j$ are simply the degrees of the network. Taking the same approach as [28] we note that in the asymptotic limit these will tend to the mean degree of the network. Consequently, for large N , the eigenvalues of L can be approximated by:

$$\mu_i \approx \kappa - \lambda_i, \quad (\text{B4})$$

where λ_i are the eigenvalues of the adjacency matrix. From this we can observe that the second smallest eigenvalues of L can be determined from the second largest eigenvalue of A .

In [28] they show that the magnitude of the Fourier coefficients is a decreasing function of the magnitude of the wavevector $|k|$ for $d = 2$. We will assume that this result extends to the case of higher dimensions. Given this, we can obtain the algebraic connectivity by computing the Fourier coefficient corresponding to $\underline{k} = (0, \dots, 0, 1)$ (or without loss of generality, any other vector for which $|k| = 1$). Furthermore, setting $\underline{k} = \underline{0}$ gives:

$$\hat{\gamma}(\underline{0}) = N \int_{\mathbb{R}^n} \gamma(\mathbf{r}) d\mathbf{r} = \kappa. \quad (\text{B5})$$

From this we see that $\mu_1 = \kappa - \kappa = 0$ which is the expected result for the Laplacian matrix.

We now consider the case of an RGG with uniform node distribution in the domain $[0, 1]^d$ with periodic boundary conditions. The periodic boundary conditions are used in order to remove boundary effects which simplifies the calculation. For an RGG with a connection radius R the connection function takes the form:

$$\gamma(\mathbf{r}) = \begin{cases} 1 & \text{if } |\mathbf{r}| \leq R, \\ 0 & \text{otherwise} \end{cases}. \quad (\text{B6})$$

Substituting this into (B3), we see that for this connection function the eigenvalues become equivalent to the Fourier coefficients of the indicator function of the ball of radius R in d dimensions. We note that this of course assumes that R is smaller than the domain size. The eigenvalues of the adjacency matrix therefore take the form:

$$\gamma(\underline{k}) = \int_{|\mathbf{r}| \leq R} e^{-2\pi i \underline{k} \cdot \mathbf{r}} d\mathbf{r}. \quad (\text{B7})$$

This integral is difficult to perform for a general \underline{k} , however, for our purposes it is sufficient to perform the integration along the d th axis of the unit ball. Setting

$\underline{k} = \underline{k}_{d,k} = (0, \dots, 0, k)$ allows us to obtain:

$$\hat{\gamma}(\underline{k}_{d,k}) = \int_{|\mathbf{r}| \leq R} e^{-2\pi i k r_d} d\mathbf{r}_1 \dots d\mathbf{r}_d. \quad (\text{B8})$$

Since the integrand now only depends on r_d we can write this integral in the form:

$$\hat{\gamma}(\underline{k}_{d,k}) = \int_{-R}^R e^{-2\pi i k r_d} \int_{r_1^2 + \dots + r_{d-1}^2 \leq R^2 - r_d^2} d\mathbf{r}_1 \dots d\mathbf{r}_{d-1} d\mathbf{r}_d. \quad (\text{B9})$$

The second integral corresponds to the volume of the sphere of radius $\sqrt{R^2 - r_d^2}$ in $d - 1$ dimensions. The volume of a d dimensional sphere of radius ρ takes the form:

$$V_d(\rho) = \frac{\pi^{\frac{d}{2}}}{\Gamma(\frac{d}{2} + 1)} \rho^d. \quad (\text{B10})$$

Therefore we obtain:

$$\hat{\gamma}(\underline{k}_{d,k}) = \int_{-R}^R e^{-2\pi i k r_d} \frac{\pi^{\frac{d-1}{2}}}{\Gamma(\frac{d-1}{2} + 1)} (R^2 - r_d^2)^{\frac{d-1}{2}} dr_d. \quad (\text{B11})$$

We now make the change of variables $r_d = R \cos(\theta)$ and set $k = 1$. After some re-arrangement we obtain:

$$\hat{\gamma}(\underline{k}_{d,1}) = \frac{\pi^{\frac{d-1}{2}}}{\Gamma(\frac{d-1}{2} + 1)} \int_0^\pi R^d \sin^d(\theta) e^{-2\pi i R \cos(\theta)} d\theta. \quad (\text{B12})$$

In order to solve this integral we make use of the following integral representation of the Bessel function of the first kind (see expression 9.1.20 on pg. 360 of [56]):

$$J_p(x) = \frac{\left(\frac{x}{2}\right)^p}{\sqrt{\pi} \Gamma(p + \frac{1}{2})} \int_0^\pi \sin^{2p}(\theta) \cos(x \cos(\theta)) d\theta. \quad (\text{B13})$$

The integral above can be split into two integrals by splitting the complex exponential into separate sin and cos terms. Noting that the second integral goes to zero due to symmetry, we obtain:

$$J_p(x) = \frac{\left(\frac{x}{2}\right)^p}{\sqrt{\pi} \Gamma(p + \frac{1}{2})} \int_0^\pi \sin^{2p}(\theta) e^{-ix \cos(\theta)} d\theta. \quad (\text{B14})$$

By comparison of (B14) and (B12) we find that:

$$\hat{\gamma}(\underline{k}_{d,1}) = R^{\frac{d}{2}} J_{\frac{d}{2}}(2\pi R). \quad (\text{B15})$$

Substitution into (B4) allows us to obtain:

$$\mu_2 \approx \kappa - N R^{\frac{d}{2}} J_{\frac{d}{2}}(2\pi R) \quad (\text{B16})$$

The techniques used to derive B16 can in principle be extended to the case of general domains and connection functions. This can be achieved by choosing the desired connection function in equation (B3) and then integrating w.r.t the desired node distribution in the corresponding domain. In many cases the resulting integral may not be tractable, however, this equation still provides some insight into the factors which effect the average value of μ_2 . Furthermore, it may be possible to extend the ideas in [54] in order to compute different eigenvalues from the spectrum of L .